5-2009

# Hydration changes of DNA binding by Klentaq and Klenow measured by Osmotic Stress

John Tod Baker

# Hydration changes of DNA binding by Klentaq and Klenow measured by Osmotic Stress

by

John Tod Baker

Undergraduate honors thesis under the direction of

Dr. Vince LiCata

Department of Biological Sciences

Submitted to the LSU Honors College in partial fulfillment of
the Upper Division Honors Program.

May, 2009

Louisiana State University
& Agricultural and Mechanical College
Baton Rouge, Louisiana

**Abstract**

The thermodynamic linkage between binding affinity and the osmotic pressure induced by non-interacting osmolytes can be used to calculate the number of water molecules bound or released during a macromolecular process such as DNA binding. For this study, osmotic stress was used to measure hydration changes associated with the DNA binding of the large fragment domains, Klentaq and Klenow, from *Taq* DNA Polymerase and *E. coli* DNA Polymerase I, respectively. Osmotic stress was performed for Klentaq and Klenow DNA binding using different osmolytes, salt conditions, DNA constructs, and temperatures. The binding affinities of both Klentaq and Klenow for DNA increases with induced osmotic pressure, which indicates a net release of water to the bulk solution upon DNA binding by these proteins. Osmotic stress performed using the osmolytes PEG 6000 and Ficoll 70,000, which are likely fully excluded from the surfaces of Klentaq and Klenow, provided estimated overall hydration changes of DNA binding of ~621 waters released for Klentaq, and ~489 waters released for Klenow. However, it is difficult to assess any true difference in hydration changes between Klentaq and Klenow DNA binding because there is overlap between the error windows on these measurements. A nonlinear relationship was observed between Klentaq DNA binding affinity and induced osmotic pressure, which results in large error windows for the linked water release of Klentaq. This was not the case for Klenow DNA binding, which exhibited a more linear relationship between binding affinity and induced osmotic pressure. At 65 ° C, Klentaq DNA binding is associated with the release of ~1266 waters, which is much higher than ~621 waters released at 25 °C. Klentaq DNA binding is entropy driven at 25 °C and enthalpy driven at 65 °C (Datta, K. and LiCata, V.J. (2003)

*Nucleic Acids Research.* **31(19)**, 5590-5597). The release of water increases the entropy of a system; however, the larger water release at 65 °C indicates that the amount of water released is not responsible for the difference in binding entropy for Klentaq DNA binding at 25 °C and 65 °C. Also, It was possible to correlate the change in solvent-accessible surface (ΔASA) calculated by osmotic stress measurements with the ΔASA calculated from X-ray crystal structures for the case of Klentaq DNA binding, but not Klenow.

## Introductory Note

The work presented in this thesis is for a current project of Dr. Vince LiCata's laboratory, which uses the osmotic stress technique to measure macromolecular hydration changes for the DNA binding of the large fragment domains of the Type I DNA polymerases from *Escherichia coli* and *Thermus aquaticus*, Klentaq and Klenow. This thesis includes includes research done by me and two graduate students, Daniel Deredge and Kausiki Datta. The initials D.D. will appear next any data obtained by Daniel Deredge, and the initials K.D. will appear next data obtained by Kausiki Datta.

## Introduction

*Taq* DNA Polymerase and *E. coli* DNA Polymerase I are a pair of thermophilic/mesophilic proteins from the Type I DNA Polymerase family. *Taq* polymerase is from the thermophilic eubacterium *Thermus aquaticus*, and *E. coli* DNA Polymerase I is from the mesophilic eubacterium *Escherichia coli*. Both polymerases have a polymerase domain, a proofreading domain, and a 5' nuclease domain (1-6). Removing the 5' nuclease domains from *Taq* Polymerase and *E. coli* DNA Pol I produces

the large fragment domains, Klentaq and Klenow respectively. Klentaq and Klenow maintain polymerase activity, and they are the subjects of interest for this study (7).

Klentaq and Klenow are very similar morphologically (Fig.1). They have almost identical three-dimensional structures and 49% sequence identity (8). Even with these similarities, there are still major functional differences between Klentaq and Klenow. In fact, the research presented in this thesis is actually part of a larger study focused on understanding the functional similarities and differences between *Taq* Polymerase and *E. coli* DNA Pol I. Unlike *E. coli* DNA Pol. I/Klenow, *Taq*/Klentaq has an inactive proofreading domain, and therefore DNA replication by *Taq*/Klentaq is a more error-prone process (1-4). However, the high thermal stability of *Taq* polymerase has made it a very important reagent in the polymerase chain reaction (PCR), because the heat denaturation of DNA can be performed at high temperatures without enzyme inactivation (8). Klentaq functions at temperatures about 40-60° higher than Klenow, which correlates with *T. aquaticus's* optimal physiological growth temperature being about ~40° higher than *E. coli's* (9). Salt dependence studies performed by Datta and LiCata on the DNA binding of Klentaq and Klenow have shown that, when binding to the same DNA, the two polymerases differ in their: binding affinities under similar solution conditions, salt tolerances, number of ions released upon binding, and requirements for bound divalent cations (10). LiCata and Datta also characterized the DNA binding of Klentaq and Klenow thermodynamically. The observed thermodynamic profiles from these studies showed that the optimal DNA binding affinity for Klentaq and Klenow occurs at different temperatures. These studies also showed similarities between the DNA binding thermodynamics of Klentaq and Klenow. DNA binding by both Klentaq

and Klenow was enthalpy driven at their respective physiological growth temperatures, and DNA binding by both polymerases exhibited a large negative heat capacity change ($\Delta C_p$) (1, 3). In an ongoing study being performed by Andy Wowor of the LiCata lab group, Klentaq and Klenow exhibited differences in their preference for binding the following DNA constructs: primed-template (pt), double-stranded (ds), and single-stranded (ss) DNA (Wowor, et al., in preparation).

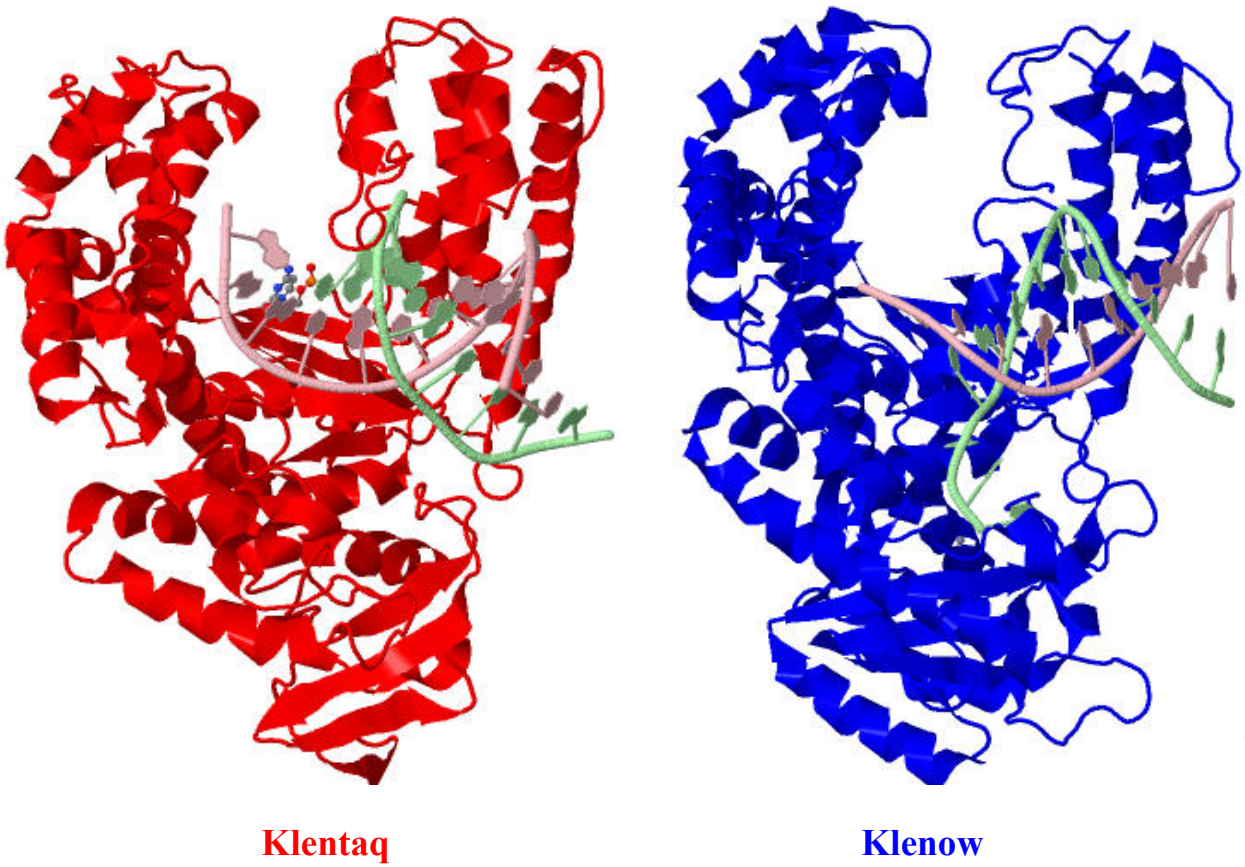


**Figure 1**: X-ray crystal structures of the large fragment domains Klentaq (PDB code 4KTQ) and Klenow (1KLN) bound to primed-template DNA.

The main focus of my research project was to measure hydration changes associated with the binding of Klentaq and Klenow to DNA. Understanding hydration changes is especially important for full comprehension of biomolecular processes that involve ligand binding and conformational changes, because these processes will involve

the release or uptake of water (13). In this study, hydration changes associated with DNA-binding were measured using a technique called osmotic stress (16).

The hydration changes osmotic stress measures are changes in solute-inaccessible water molecules associated with a change between two macromolecular forms. Large polymers that are added to a solution of macromolecules can be excluded from regions of the macromolecules such as surface crevices and internal cavities (Fig. 2). These regions will be inhabited by water molecules that are inaccessible to the polymers in the bulk solution. Since water tends to move down its concentration gradient through osmosis, the large polymers, or "osmolytes," osmotically stress the solute-inaccessible waters associated with the macromolecule (16) (Fig. 2). Therefore, when the osmotic pressure, or $\prod$, of the bulk solution is increased by adding osmolytes, movement of water away from solute-inaccessible regions of a macromolecule is favored. By increasing the $\prod$ of a solution, macromolecular processes involving the release of water to the bulk solution will be favored, and macromolecular processes involving the uptake of water from the bulk solution will be inhibited. The osmotic stress technique uses this shift in equilibrium of a macromolecular process with induced $\Pi$ to calculate the change in solute-inaccessible waters associated with that process (13). When this relationship between equilibrium and $\Pi$ is evaluated empirically, the data can be analyzed to provide a thermodynamic water linkage plot. The application of the osmotic stress technique will be described in more detail in the Materials & Methods.

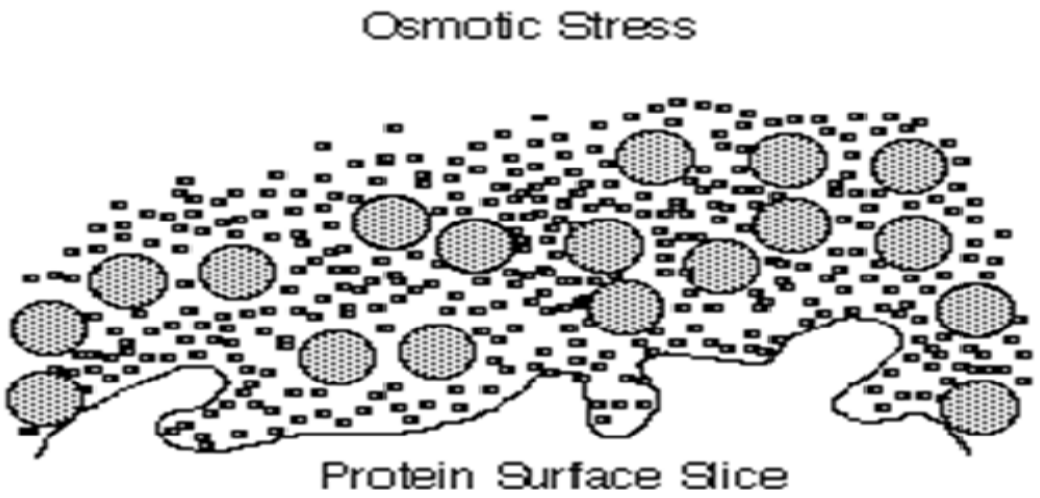


**Figure 2**: Schematic representation of a protein surface under osmotic stress. The large, gray spheres represent solute molecules that are excluded from regions of the protein surface. The small black ovals represent water molecules. Waters that inhabit the solute-inaccessible regions of the surface are osmotically stressed by the large solutes (osmolytes) due to the higher concentration of water in these regions relative to the bulk solution (13).

This thesis presents hydration changes measured for Klentaq and Klenow DNA binding under various solution conditions. The solution conditions that were varied include the identity of the osmolyte, the presence of additional small solutes (salts), and the DNA construct used. Hydration changes for Klentaq were also measured at different temperatures. By using different solution conditions, a range of values for the change in solute-inaccessible waters associated with binding was determined. Some of these values were deemed to be the best estimates of the overall hydration changes for binding because they likely provide information about water movement from the largest, solute-inaccessible regions of the proteins (13). It was found that compared to other DNA binding proteins for which similar measurements exist, both Klentaq and Klenow release

a large amount of water to the bulk solution upon binding to primed-template DNA (pt-DNA). Reasons for why certain solution conditions altered the number of waters released is also discussed. Estimates of the overall hydration change for Klentaq and Klenow were also used to calculate the change in solvent-accessible surface (ΔASA), and this ΔASA calculated from the overall hydration change was compared with the ΔASA calculated from the X-ray crystal structures of polymerases and polymerase-DNA complexes. However, the discrepancy between osmotic stress-based and structure-based calculations could be resolved for Klentaq by accounting for the number of non-surface bound waters within the binding cleft measured by osmotic stress.

## Materials & Methods

### Proteins

The proteins examined in this study were the large fragment domains, Klentaq and Klenow, of *Taq* DNA polymerase I and *E. coli* DNA polymerase I, respectively. Purified proteins were dialyzed into storage buffer or a buffer for experimentation by dialyzing them against 4 large volume changes of the desired buffer over a total of 16 hours. The concentrations of these enzymes were measured on a Cary100 spectrophotometer at 280 nm.

### DNA

The DNA constructs used for binding assays were the following:

13/20 mer

5'–TCGCAGCCGTCCA- 3'
3'-AGCGTCGGCAGGTTCCCAAA-5'

63/70 mer

5’-TACGCAGCGTACATGCTCGTGACTGGGATAACCGTGCCGTTTGCCGATTTCGCAGCCGTCCA-3’
3’-ATGCGTCGCATGTACGAGCACTGACCCTATTGGCACGGCAAACGGTGAAAGCGTCGGCAGGTTCCCAAA-5’

20/20 mer

5’-TCGCAGCCGTCCAAGGGTTT-3’
3’-AGCGTCGGCAGGTTCCCAAA-5’

All were labeled fluorescently with a Rhodamine-X fluorophore so that equilibrium titrations with DNA and protein could be monitored by fluorescence anisotropy (32, 33).

**Calculations for hydration changes and equilibrium titrations monitored by fluorescence anisotropy**

For this study, the osmotically induced shift in equilibrium for Klentaq/Klenow binding to DNA was monitored by performing equilibrium enzyme-DNA titrations. As the enzyme concentration was varied, the amount of enzyme-DNA complex present was detected by measuring the fluorescence anisotropy of the solution with a Fluoromax-2 fluorometer. The data was then fit to a single-site binding isotherm using the equation:

$$\mathbf{\Delta A = \{\Delta A_T(E_T/K_d/)/(1+E_T/K_d)\}}$$

where $\Delta A$= the change in anisotropy, $\Delta A_T$= total change in anisotropy, $E_T$=enzyme concentration at a point, and the $K_d$=dissociation constant.

Performing a series of equilibrium titrations under differ osmotic pressures provided empirical values for dissociation constants ($K_d$) of binding, which could be related to the osmotic pressure they were measured at by the equation:

$$\frac{\partial kT\ln(K^{\Pi}/K^{0})}{\partial \prod_{osm}} = \Delta V_w = \Delta N_w \text{ X } 30 \text{ Å}^3 \quad \textbf{Eq. 1}$$

Where $K^{\Pi}$ is the dissociation constant ($K_d$) at each osmotic pressure $\prod_{osm,}$ $K^0$ is the $K_d$ in the absence of added osmolyte, $\Delta V_w$ is the linked change in water volume, 30 $Å^3$ is the volume of single water molecule, $\Delta N_w$ is the linked change in the number of

associated waters, k is Boltzmann's constant, and T is temperature (4). Plotting $kTln(K^{\Pi}/K^{0})$ vs. $\Pi$ provides a thermodynamic water linkage, which can be fitted to a line. The slope correspondes to the $\Delta V_{w,}$ and $\Delta N_w$ is calculated by dividing $\Delta V_w$ by the molecular volume of a single water molecule (30 $Å^3$).

Equilibrium titrations were performed by titrating Klentaq or Klenow into 1nM Rhodamine-X-labeled DNA in salt solutions buffered with 10 mM Tris at pH 7.9 that contained various concentrations of an osmolyte (0-30% (w/v) osmolyte). The DNA solution was always 2 mL and in a quartz cuvette, and a magnetic stir bar was used to continuously stir the solution. The DNA solution and the enzyme titrant added contained the same solute concentrations (both osmolytes and salts). The value of $K^0$ was measured in the base buffer, which was the Tris-buffered salt solution without any added osmolyte (0% (w/v) osmolyte), and the values of $K^{\Pi}$ were measured as different amounts of osmolyte were added to the base buffer. For osmotic stress measurements on Klentaq, the salt conditions for the base buffer were one of the following: 1) 125 mM KCl; 2)125 mM KCl and 5 mM $MgCl_2$; 3) 100 mM KCl; 4) 100 mM KCl and 5 mM $MgCl_2$; 5) 250 mM KGlu; 6) 125 mM KCl and PEG 200. For the osmotic stress measurements on Klenow, the salt conditions were either 1) 500 mM KCl or 2) 800 mM KGlu. The $\prod$ of these base solutions was varied by diluting 30 % (w/v) osmolyte stock solutions with a base buffer. The 30% (w/v) osmolyte stock solutions were prepared by adding the appropriate mass of osmolyte to the base buffer. The polymers used as osmolytes in this study were various molecular weight ($M_w$) polyethylene glycols (PEG) and dextrans, and a Ficoll polymer of $M_w$ 70,000. The $\Pi$ of solutions was measured using a Wescor vapor pressure osmometer (VPO).

All titrations were performed at 25 ºC with the exception of one set of titrations for Klentaq performed at 65 ºC. For the titrations at 65 ºC, 63/70 mer DNA had to be used because 13/20 mer DNA would melt at this temperature.

**DNA volume calculations from the x-ray crystal structures**

In an effort to correlate between molecular calculations from osmotic stress and X-ray crystallography presented later in this thesis, the volume of solute-inaccessible, non-surface bound water displaced from free polymerase by incoming DNA was calculated from published X-ray crystal structures. The structure-based calculations were based on x-ray crystal structures of the Klentaq and Klenow large fragments bound to primer-template DNAs similar to that used for this study (PDB code 4KTQ and 1KLN respectively). PDB files were analyzed at the CASTp database online (Computer Atlas of Surface Topography of Protiens) (14). When Klentaq and Klenow bind DNA, surface- and non-surface bound water is displaced by the incoming DNA. The amount of solute-inaccessible, non-surface associated water displaced can be evaluated by approximating the volume of DNA located in solute inaccessible regions of the DNA bound polymerase complex. Portions of bound DNA that extend into solute-accessible regions of the solution are not included in the calculations.

The amount of DNA that extends into solute-accessible regions was evaluated by approximations of the thickness of the preferential hydration shell based on work done by Bhat and Timasheff. Using high precision densimetry, Bhat and Timasheff measured the preferential interactions of several proteins, that vary in molecular weight and surface polarity, with PEG 2,000-6,000. Then, using a model for proteins with assumed spherical shape, Bhat and Timasheff related the average thickness of the preferential hydration

shell, defined as the radius of exclusion, $R_e$, to the measured preferential hydration with PEG. The radius of exclusion ($R_e$) extends from the center of the spherical protein, and sweeps out a volume that is impenetrable to the osmolyte (See Fig. 3). Values for the protein radius and radius of exclusion for proteins assumed to have a spherical shape are listed in Table 1. These values were derived from solutions of the primary osmolyte used in this study, PEG 6000 (15). In this study, the difference between the $R_e$ and $R_p$ values for each protein in Table 1 were averaged to provide an approximate distance from the Klentaq/Klenow surface to the edge of the solute-inaccessible region. The average distance used was 17 Å. It was found that only about 1 nucleotide was located farther than 17 Å from the surface of Klentaq, and the volume of this nucleotide was excluded from DNA volume calculations with Klentaq. None of the DNA was located farther than 17 Å from the surface of Klenow, and therefore no nucleotides were exclude from DNA volume calculations with Klenow.

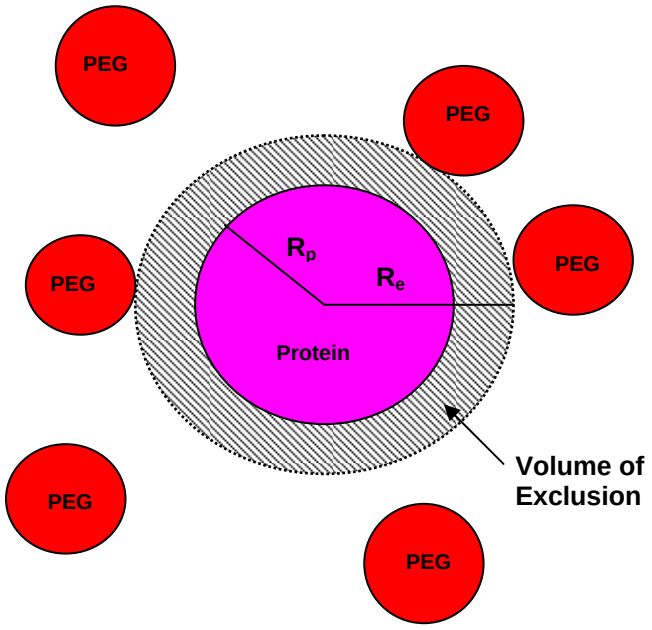


**Figure 3:** Schematic representation of the preferential hydration of a protein with PEG. The radius of exclusion ($R_e$) extends from the center of the spherical protein, and sweeps out a volume that is impenetrable to the osmolyte. Subtracting the radius of the protein ($R_p$) from the $R_e$ is equal to the distance from the surface of the protein that PEG is excluded. To determine the number of solute-inaccessible waters displaced by the volume of the DNA for the DNA binding of Klentaq and Klenow, it was necessary to determine if any of the bound DNA extends into regions that are accessible to PEG, because DNA extending into PEG accessible regions would have only displaced solute-inaccessible waters.

**Table 1**

| Protein | $R_p$(Å) | $R_e$(Å) | Rp-Re(Å) |
|---|---|---|---|
| BSA | 27 | 39.1 | 12.1 |
| Chymotrypsinogen | 19.5 | 29.2 | 9.7 |
| Lysozyme | 15.8 | 39.9 | 24.1 |
| β-LG | 18 | 40.3 | 22.3 |
| RNAse A (pH 2) | 15.5 | 34.7 | 19.2 |

**Table 1**: Table of the radii of exclusion ($R_e$) towards PEG 6000 for several proteins derived from the proteins' assumed spherical shape with radius $R_p$. The differences between the the radii of exclusion and the radii of the protein ($R_p$) provide a distance from the protein surface that excludes PEG 6000 (15).

In the X-ray crystal structures used to calculate DNA volumes, Klentaq and Klenow are bound to primed-template DNAs which have an approximately double-helical region and an irregularly shaped single-stranded overhang (Fig. 4). The double-helical portion of the bound-DNAs in the crystal structures was assumed to be cylindrical, and the equation $V_{DNA}=\pi r^2 h$ was used to calculate the solute-inaccessible volume of double-helical DNA. The approximate height and diameters of the DNAs were determined by measuring distances between atoms on the double-helix using CASTp (See Figure 4). In the DNA-bound crystal structures of Klentaq and Klenow, the single-stranded regions of the bound DNAs make a much smaller contribution to the total DNA volume than the double-helical regions. For both the Klentaq and Klenow structure, only the volume of 3 nucleotides couldn't be included in the double-helical volume calculations. One of these 3 nucleotides for the DNA bound to Klentaq, was actually not part of a single DNA strand, but was instead the nucleotide remaining after removal of the one solute-accessible nucleotide. Adding the approximate volumes of the 3 individual nucleotides to the double-helical volumes provided a DNA-displaced volume of solute-inaccessible water of ~9738 $Å^3$ for DNA binding to Klentaq and ~9774 $Å^3$ for DNA binding to Klenow. Dividing these volumes by the volume of a single water

molecule of 30 Å$^3$, results in a calculated displacement of ~325 waters by the DNA for both Klentaq and Klenow.

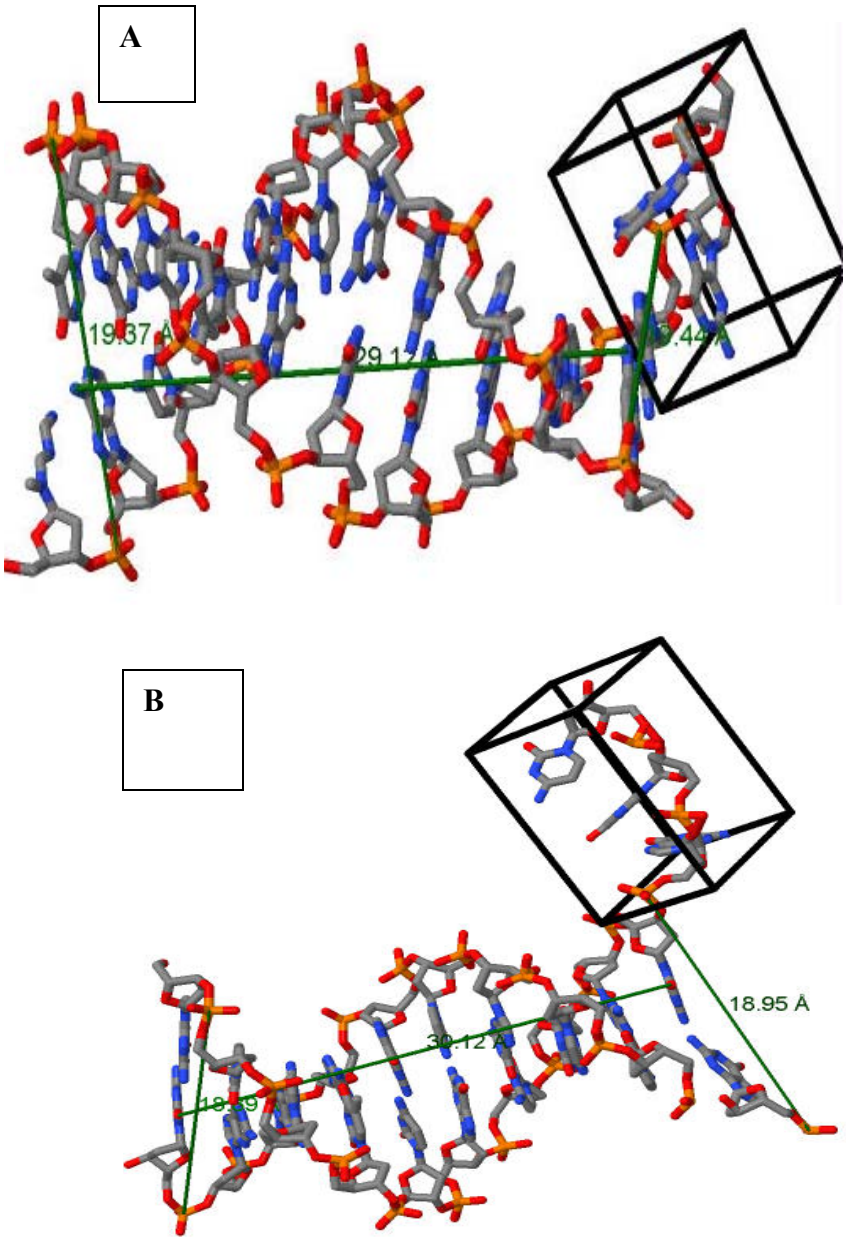


**Figure 4:** X-ray crystal structures of primed-templated DNAs while bound to Klentaq (**A**) and Klenow (**B**). The structures for Klentaq and Klenow were removed in CASTp, and therefore don't appear in the figures. The dimensions of these structures were determined to provide approximations of the volume of solute-inaccessible, non-surface associated water displaced by DNA during binding. The pt-DNAs have an approximately double-helical region and an irregularly shaped single-stranded overhang. The double-helical portion of the DNAs was assumed to be cylindrical, and the equation $V_{DNA}=\pi r^2 h$ was used to calculate the volume of this portion. For the bound DNA in both **A** and **B,** the diameter is the average between the two lines connecting phosphates at either the primer-template junction or the end opposite to it. The average diameter of the DNA was 19.41 Å for **A** and 18.92 Å for **B**. The height of the double-helix in **A** was determined to be 29.12 Å, by measuring the distance between the N6 of an adenine in the 2$^{nd}$ base-pair at the blunt end, and the N4 of a cytosine in the basepair at the primer-template junction. Since one nucleotide of the bound-DNA in the Klentaq crystal structure was solute-accessible, it was removed from the DNA structure (left side of DNA in A). The height of the double-helix in **B** was determined to be 30.12 Å by measuring the distance between the O2 of a cytosine in the basepair at the primer-template junction, and the O2 of a cytosine in the basepair at the blunt end. The volume of the single-stranded portions were approximated by using a feature in CASTp that just perfectly encloses molecular models in a "boundbox" and calculates the volume of the box (Black boxes in **A** and **B**) (5). The 2 base pair template overhang for **A** has a volume of ~933 Å$^3$, while the 3 base pair template overhang in **B** has a volume of ~1305 Å$^3$. The volume of the nucleotide that was base-paired with the solute-accessible nucleotide for the Klentaq crystal structure (**A**) was also calculated by the boundbox method (not shown) and resulted in a volume of ~189 Å$^3$. The volumes of both double-helical and single-stranged-DNA were added together to provide DNA volume of ~9738 Å$^3$for the Klentaq structure (**A**) and ~9774 Å$^3$ for the Klenow structure (**B**) (14).

# Results

## Solute Size Dependence

If the overall hydration change for a macromolecular process is to be determined by osmotic stress, then "neutral" osmolytes must be chosen that are excluded from all differentially hydrating spaces on macromolecules participating in the process (13). This means these osmolytes must be excluded from internal cavities, surface crevices, and surfaces well-exposed to the bulk. Many solutes are excluded sterically from spaces because they are too large to fit. Surfaces well-exposed to the bulk solution can also exclude solutes through a preferential hydration mechanism. In the case of preferential hydration, solutes have an unfavorable chemical interaction with the exposed surface compared to the interaction of water. Therefore, if neutral osmolytes are used, then a large number of regions on a macromolecule can be probed by osmotic stress because they are likely inhabited by solute-inaccessible water. This makes it important to consider both the size and the chemical nature of osmolytes when designing osmotic stress experiments (13, 16).

Prior to performing osmotic stress, solute size dependence experiments can determine which osmolytes are excluded from internal cavities and surface crevices. These experiments may be sufficient to find the proper osmolytes for probing the dimensions of spaces such as channels, where different-sized solutes can or cannot enter (16). However, the chemical nature of osmolytes becomes especially important when investigating protein-DNA interactions by osmotic stress because many of the important surfaces involved are well-exposed to the bulk solution. Some osmolytes may interact with the well-exposed surfaces of the protein and DNA. Also, osmolytes may have other

effects on the solution such as changing the dielectric constant or pH. Therefore, osmolytes must be evaluated to ensure that they act primarily to alter the $K_d$ by changing $\Pi$, and not by some other effect specific to a particular osmolyte. Mechanisms of solute action would be expected to vary with the chemical nature of the solute; therefore, several measurements of hydration changes using chemically different osmolytes can be compared to determine if those osmolytes are altering the $K_d$ by some specific effect in addition to altering $\prod$ (16). For the osmotic stress of Klentaq and Klenow in this study, solute size dependencies were examined, and hydration changes were measured using several chemically different osmolytes.

The solute size dependence experiments for Klentaq and Klenow assessed which sizes of a homologous series of high-molecular weight polymers would be excluded from all the differentially hydrating spaces (13,16). Two homologous series were utilized: polyethylene glycols (PEG, from $M_w$ 200 to 10,000) and dextrans (from $M_w$ 1500 to 20,000). For the curves in Figure 5, the data points represent dissociation constants ($K_d$) for DNA binding at the same osmotic pressure induced by different $M_w$ polymers of a homologous series (Table 2 and Fig. 5). The osmotic pressure is kept the same by adjusting the %(w/v) in solution of each $M_w$ polymer appropriately. For example, the % (w/v) of higher $M_w$ PEG would be increased to give the same osmotic pressure of a lower $M_w$ PEG because osmotic pressure is dependent upon the number of particles in solution (Table 2). When the measured $K_d$ becomes constant regardless of polymer size, a solute size plateau occurs consisting of increasingly large $M_w$ polymers that are excluded from a constant region of the macromolecule (Fig. 5). Prior to the plateau, the binding becomes tighter with increasing exclusion of polymer and consequent increase in solute

inaccessible waters associated with the protein. This shows that DNA binding by both polymerases involves a net release of waters to the bulk solution because processes involving release of water to the bulk solution are favored by high Π. A net release of water is expected for protein-DNA interactions, in which water is displaced from the surfaces of protein and DNA (16).

The PEG size dependencies for both Klentaq and Klenow plateau near PEG 5000. This means PEGs of $M_w$ 5000 and above all stress the same macromolecular regions for each individual protein (Fig. 5). PEG 6000 was chosen as a stressing osmolyte in this study, which is a good choice for osmotic stress of Klentaq and Klenow for several reasons. PEG 6000 is easier to work with than higher $M_w$ PEGs, and its similar exclusion to that of larger PEGs ensures it will stress large, spaces that are likely to be functionally significant such as solute-inaccessible pockets located on the DNA binding sites of Klentaq and Klenow. Also, PEG 6000's binding interaction with the surfaces of the polymerases is probably not significant. Preferential hydration studies by Timasheff and associates showed that PEGs of $M_w$ 200-6,000 are strongly excluded from the surfaces of many proteins varying in hydrophilic/hydrophobic character (15). The preferential hydration for these studies was highest in solutions of PEG 6000 (15). Despite all of these characteristics, it was still necessary to compare the hydration changes measured with PEG 6000 to that of other chemically different osmolytes to make sure PEG 6000 acts primarily to alter the $K_d$ by altering Π. This was done by comparing the hydrations changes measured by PEG 6000 to measurements with Ficoll 70,000. A solute size dependence was not performed for Ficoll polymers because Ficoll 70,000 is considered to

be large enough to probe hydration changes of macromolecular surfaces and has been used extensively for this purpose by Bloomfield and coworkers (17).

**Table 2: PEG Solute Size Dependence for Klenow binding to 13/20 mer DNA**

All titrations were performed at 28.49 atm osmotic pressure. Similar solute size dependence tables for Klentaq binding to 13/20 mer DNA are not shown here, and are presented in Kausiki Datta's (K.D.) dissertation. The base buffer salt was 500 mM KCl.

| Nature of osmolyte | Concentration of osmolyte %(w/v) | $K_d$ (nM) |
|---|---|---|
| No osmolyte | 0 | 183.6 (+/-) 12 |
| PEG 200 | 3.2 | 80.4 (+/-) 10.9 |
| PEG 1000 | 7 | 40.0 (+/-) 6.4 |
| PEG 3000 | 9 | 21.4 (+/-) 3.8 |
| PEG 6000 | 10 | 18.9 (+/-) 2.3 |
| PEG 8000 | 10 | 17.9 (+/-) 3.4 |
| PEG 10,000 | 10 | 17.6 (+/-) 3.7 |

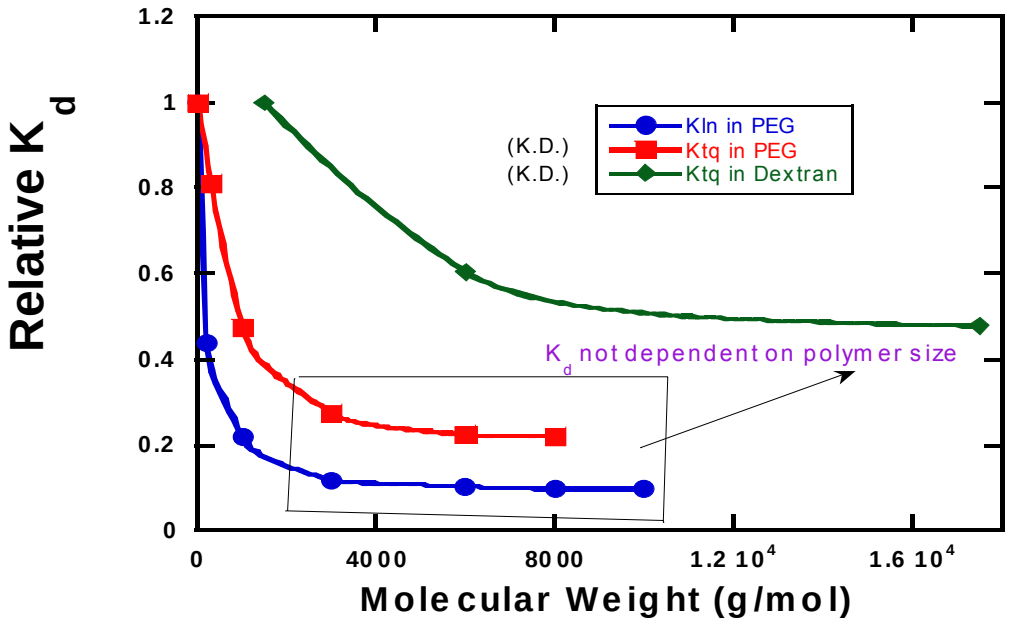


**Figure 5:** Solute size dependencies for Klentaq in PEG and Dextran, and for Klenow in PEG. The shift in equilibrium of DNA binding due to the addition of increasingly large PEG size is monitored at a constant osmotic pressure. The range of polymer sizes for which this shift stops occurring provides the potential osmoltye size range appropriate for osmotic stress studies. The solute size plateau begins < 5000 $M_w$ PEG for both Klentaq and Klenow.

**Osmotic stress of the DNA binding of Klentaq at 25 ºC**

Figures 6 & 7 show thermodynamic water linkages for the DNA binding of Klentaq, and the changes in solute-inaccessible waters associated with binding ($\Delta N_w$ values) are tabulated in Table 3. All water linkages in this thesis show the binding affinity of Klentaq and Klenow for DNA increasing with induced $\prod$. Therefore, all $\Delta N_w$ values presented in this thesis correspond to the net release of water to the bulk solution. The $\Delta N_w$ values for Klentaq showed variance among the different solution conditions that they were measured under (DNA construct, salt, osmolyte, temperature) (Table 3). However, when Klentaq was osmotically stressed with either PEG 6000 or Ficoll 70,000 in KCl in the presence or absence of $Mg^{2+}$ , the same number of waters were released upon binding of 13/20 mer DNA (Figure 6 and Table 3). The similarity observed between measurements with these chemically different osmolytes shows that neither osmolyte is interacting specifically with the protein, and that they are acting primarily to alter the $K_d$ by altering $\prod$ (13). Therefore, these large osmolytes are likely probing many large hydration spaces on Klentaq that they are excluded from either sterically or through a preferential hydration mechanism (16). Consequently, the first four $\Delta N_w$ values listed in Table 3 were averaged together to obtain an estimate for the overall hydration change associated for the 13/20 mer DNA binding of Klentaq (Fig. 6). The average of these four values indicates that Klentaq releases ~621 waters to the bulk solution upon binding to pt-DNA.

Some caution must be taken when interpreting the hydration changes for Klentaq because of the apparent nonlinearity of the water linkages (Fig 6). The nonlinearity is also a major source of the large error for many of the $\Delta N_w$ values measured for Klentaq.

The nonlinearity cannot currently be explained, but non-linear fits or adjustments to experimental procedures could change the interpretation of the results for osmotic stress of Klentaq.

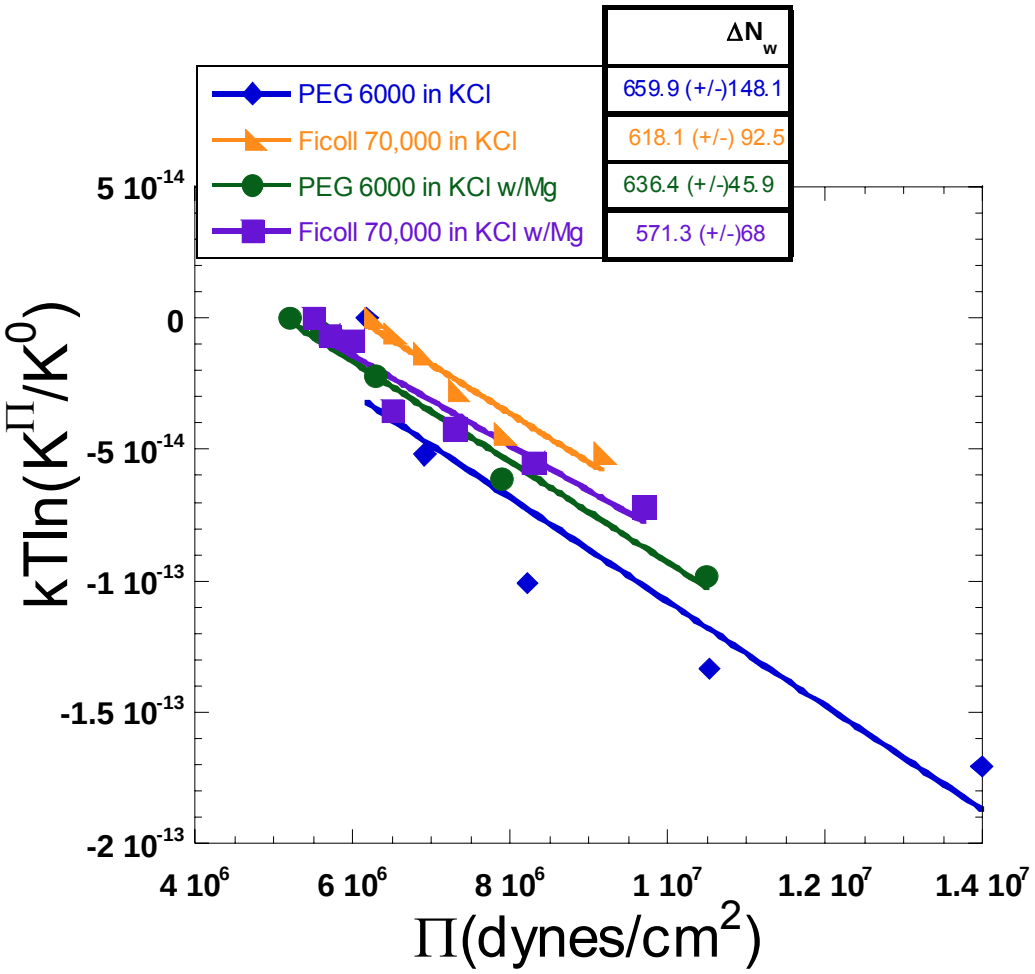


**Figure 6:** Thermodynamic water linkages for the 13/20 mer DNA binding of Klentaq under osmotic stress with PEG 6000 or Ficoll 70,000 in a base buffer containing KCl in the presence or absence of $Mg^{2+}$. The increase in binding affinity, which is represented by a decrease in $kTln(K^{\Pi}/K^{0})$, with induced Π indicates that there is a net release of solute-inaccessible waters to the bulk solution when binding occurs. The slopes translate into large magnitudes for $\Delta N_w$, which all agree statistically, but the lines are fit to an apparent nonlinear relation. The $\Delta N_w$ values listed in the figure were averaged to obtain the best estimate for the overall hydration change for pt-DNA binding of Klentaq. The $\Delta N_w$ values in the figure are listed next to and color-coded to the solution conditions they were measured under, which are presented in the legend as: Osmolyte in KCl with or without $Mg^{2+}$. Base buffers made without 5 mM $Mg^{2+}$ contained 125 mM KCl, while those made with 5 mM $Mg^{2+}$ contained 100 mM KCl.

Performing osmotic stress under some solution conditions reduced the hydration change measured for Klentaq. There is a large reduction in the $\Delta N_w$ for measurements made with Dextrans (Table 3 & Figure 7). Measurements made with both Dextran 6000 and 15,000-25,000 indicate a net release of ~240-250 waters for 13/20 mer DNA binding of Klentaq (Table 3). The similarity between $\Delta N_w$ values measured with Dextrans 6000 and 15,000-25,000 may indicate fully sized-based exclusion for these osmolytes, but the large discrepancy between $\Delta N_w$ values measured with Dextrans and PEG 6000 or Ficoll 70,000 suggests that Dextran interacts specifically with the protein (Table 3 and Figure 7). Therefore, Dextran should not be used to probe overall hydration changes for Klentaq. Also, the $\Delta N_w$ measured with PEG 200 is only 121 (+/-) 8.1 (Table 3 & Fig.7), which demonstrates the importance of using only osmolyte sizes from the solute size plateau (Fig. 5). In the presence of 250 mM KGlu salt, the $\Delta N_w$ measured with PEG 6000 is only 253.8 (+/-) 31 (Fig. 7 & Table 3). This shows that glutamate acts specifically on Klentaq. Interestingly, the $\Delta N_w$ measured with PEG 6000 in the presence of 250 mM PEG 200, which has $M_w$ similar to glutamate, didn't seem to differ significantly from the $\Delta N_w$ measured with PEG 6000 in the presence of KCl (Fig. 7 & Table 3). This indicates that glutamate's behavior in solution deviates largely from the behavior of a pure 200 $M_w$ osmolyte.

Hydration changes for Klentaq binding to 13/20 mer DNA are within error of the hydration changes measured for binding to 20/20 mer DNA double-stranded DNA (Figure 8). However, if the error in the $\Delta N_w$ values can be reduced, than a significant difference in released water may be seen between pt- and ds-DNA binding.

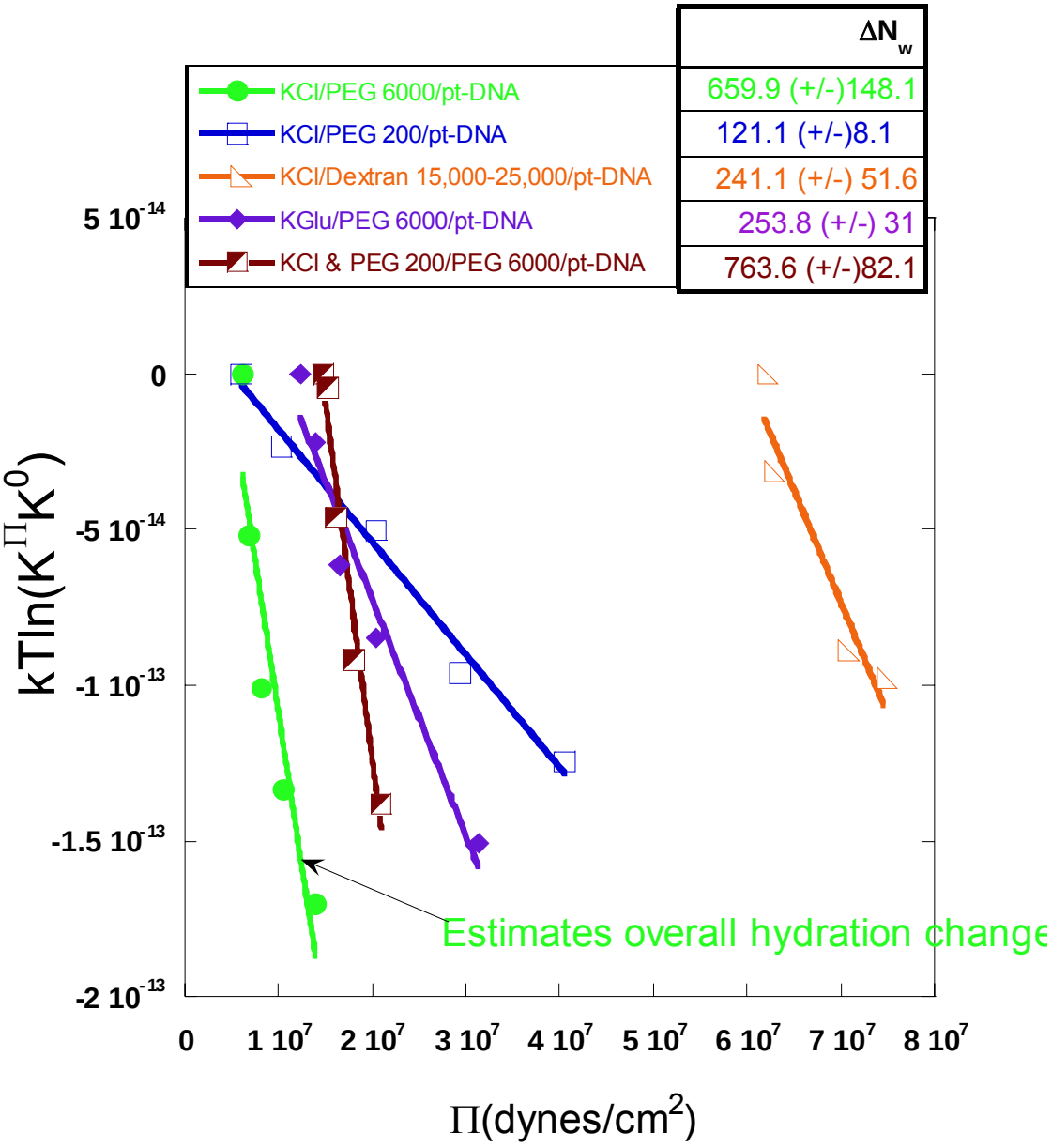


**Figure 7:** Thermodynamic water linkages for the 13/20 mer DNA binding of Klentaq under various solution conditions. Conditions are listed in the legend are listed in the legend as: salt/osmolyte/DNA. The $\Delta N_w$ values are listed next to and color-coded to the solution conditions they were measured under. The KCl and KGlu concentrations used for the linkages in this figure are 125 mM and 250 mM, respectively. The lime green water linkage plot corresponds to measurements made with PEG 6000 in KCl and the slope translates into a good estimate of the overall hydration for pt-DNA binding of Klentaq. The use of both PEG 200 and Dextran 15,000-25,000 as osmolytes drastically reduces the $\Delta N_w$. The use of 250 mM glutamate salt also reduces the $\Delta N_w$, but using 250 mM PEG 200, which has a $M_w$ similar to glutamtate, does not reduce the $\Delta N_w$.

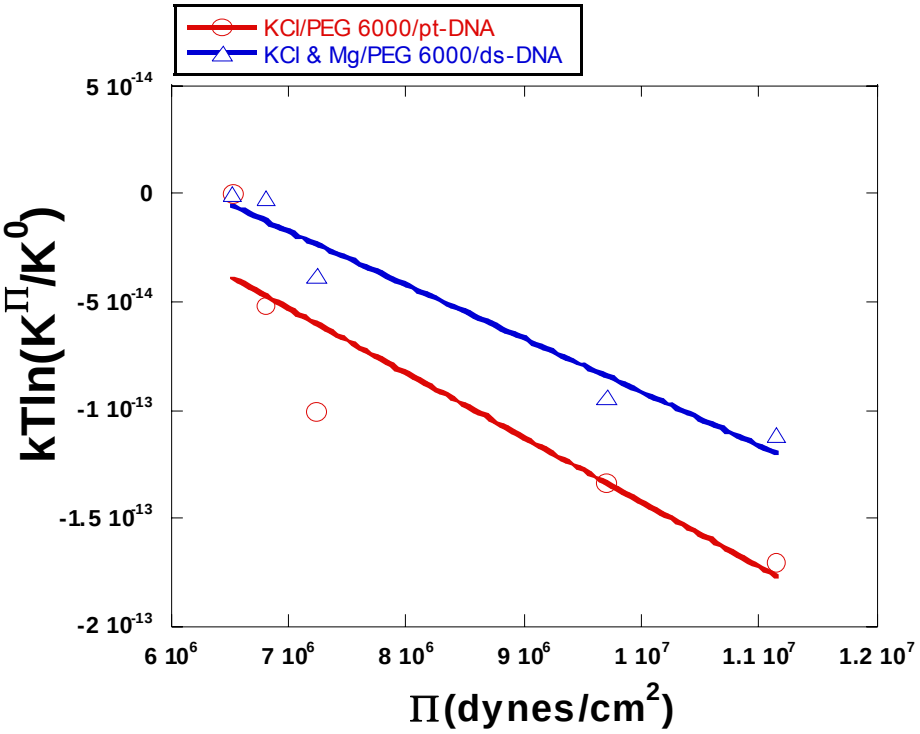


**Figure 8:** Water linkages for Klentaq binding to pt-DNA and ds-DNA. The slopes appear to be close, but the $\Delta N_w$ values have large errors, and thus it is difficult to tell whether there is a significant difference in the hydration change for these two DNA constructs.

**Table 3: $\Delta N_w$ values for the DNA binding of Klentaq**

| DNA (mer) | Salt(s) | Osmolyte | $\Delta N_w$ |
|---|---|---|---|
| 13/20 | 125 mM KCl | PEG 6000 | 659.9 (+/-)148.1 |
| 13/20 | 125 mM KCl | Ficoll 70,000 | 618.1 (+/-) 92.5 (D.D) |
| 13/20 | 100 mM KCl, 5 mM $MgCl_2$ | PEG 6000 | 636.4 (+/-)45.9 (K.D) |
| 13/20 | 100 mM KCl, 5 mM $MgCl_2$ | Ficoll 70,000 | 571.3 (+/-)68 (K.D.) |
| 13/20 | 125 mM KCl | PEG 200 | 121.1 (+/-)8.1 |
| 13/20 | 100 mM KCl, 5mM $MgCl_2$ | Dextran 6000 | 249.5 (+/-)16.5 (K.D.) |
| 13/20 | 125 mM KCl | Dextran 15,000-25,000 | 241.1 (+/-) 51.6 |
| 13/20 | 250 mM KGlu | PEG 6000 | 253.8 (+/-) 31 |
| 13/20 | 150 mM KCL, 250 mM PEG 200 | PEG 6000 | 763.6 (+/-)82.1 |
| 20/20 | 125 mM KCl, 5 mM $MgCl_2$ | PEG 6000 | 827 (+/-) 109 |
| 63/70 (*65° C) | 125 mM KCl, 5 mM $MgCl_2$ | PEG 6000 | 1448 (+/-) 132.8 (non-synergistic), 1084 (+/-) 146.5 (synergistic) |

**Osmotic Stress of the DNA binding of Klenow at 25 ºC**

Osmotic stress was also performed for 13/20 mer DNA binding by Klenow by Daniel Deredge (D.D.) (Figure 9 & Table 4). The $\Delta N_w$ values for Klenow measured with PEG 6000 and Ficoll 70,000 in KCl agree with one another. The two $\Delta N_w$ values measured with PEG 6000 and Ficoll 70,000 were averaged to obtain an estimate of the overall hydration change for pt-DNA binding of Klenow of a net ~489 waters released upon binding. The overall hydration change for Klenow was estimated in this way for the same reasons the overall hydration change for Klentaq was estimated with measurements using PEG 6000 and Ficoll 70,000 in KCl. Some of the solution conditions that reduced the $\Delta N_w$ measured for the DNA binding of Klentaq, also reduced the $\Delta N_w$ measured for the DNA binding of Klenow (Table 4 and Fig.9 ). For the DNA binding of Klenow measured with PEG 200 as an osmolyte, the $\Delta N_w$ was 104.9 (+/-) 10.3. The increase in $\Delta N_w$ for measurements with PEG 1000 compared to PEG 200 indicates that the greater exclusion of the larger PEG 1000 results in more water being osmotically stressed (Table 4 and Fig.9 ). These results with PEG 200 and PEG 1000 demonstrate the importance of using PEG sizes from the solute size plateau, as did the results from using PEG 200 as a stressing agent with Klentaq (Fig. 5 and Table 4). In the presence of 800 mM KGlu, the $\Delta N_w$ measured with PEG 6000 is only 145.9 (+/-) 13.6 Fig. 9 and Table 4). As with Klentaq, glutamate appears to act specifically on Klenow. These results with glutamate salts for Klentaq and Klenow are part of larger study by Daniel Deredge concerning how glutamate influences DNA-protein interactions both osmotically and ionically.

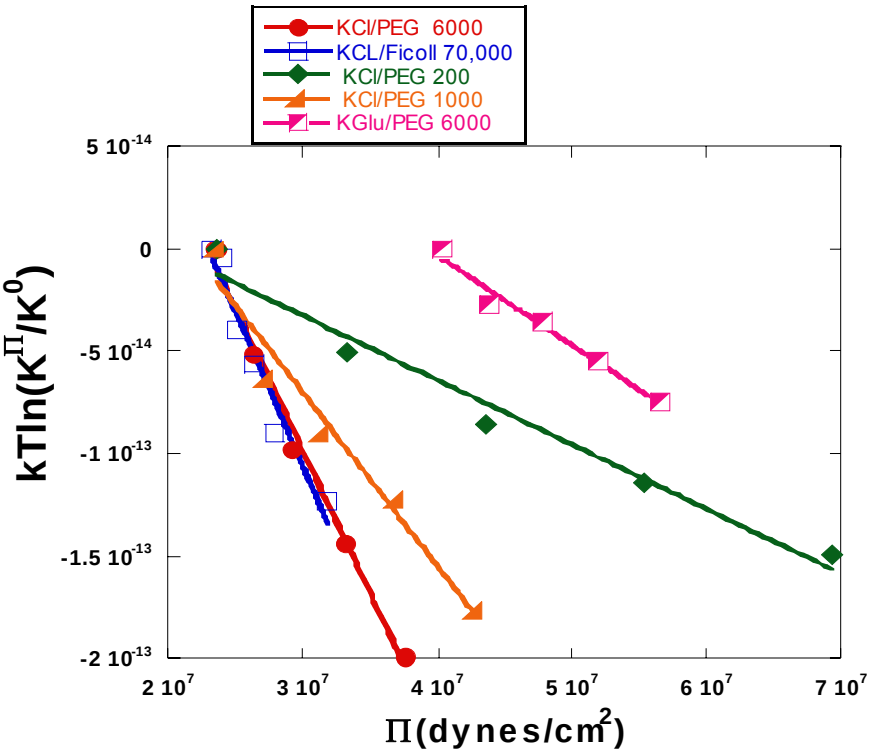


**Figure 9:** Thermodynamic water linkages for Klenow binding to pt-DNA under various solution conditions. Conditions are presented in the legend as salt/osmolyte. The salt concentration was either 500 mM KCl or 800 mM KGlu.. All experiments for Klenow were performed at 25 °C. See Table 4 below for $\Delta N_w$ values. Note the agreement in slopes for the red and blue lines which represent experiments done with PEG 6000 and Ficoll 70,000 respectively. There is also a higher degree of linear character in the plots, which is reflected in the lower error of the $\Delta N_w$ values. All plots by Daniel Deredge.

**Table 4: ΔNw values for the DNA binding of Klenow. All experiments were performed with 13/20 mer DNA at 25° C. Data from Daniel Deredge.**

| Salt(s) | Osmolyte | ΔNw |
|---|---|---|
| 500 mM KCl | PEG 6000 | 460.6 (+/-) 20.3 |
| 500 mM KCl | Ficoll 70,000 | 516.9 (+/-) 53 |
| 500 mM KCl | PEG 200 | 104.9 (+/-) 10.3 |
| 500 mM KCl | PEG 1000 | 281.9 (+/-) 31.3 |
| 800 mM KGlu | PEG 6000 | 145.9 (+/-) 13.6 |

**Comparison between hydration changes of Klentaq and Klenow**

Without considering the error for $\Delta N_w$ values, the $\Delta N_w$ values for pt-DNA binding of Klentaq are significantly larger than the corresponding values for Klenow. However, the large error windows on the $\Delta N_w$ values for Klentaq overlap with many of the error windows on the $\Delta N_w$ values of Klenow (Table 3, Table 4, Fig. 10). Therefore, the hydration changes measured for this study indicate that Klentaq and Klenow statistically release the same number of waters upon binding to pt-DNA. However, higher precision data for Klentaq that decreases the error windows could reveal significant differences between the hydration changes for Klentaq and Klenow binding to DNA. Resolving issues concerning the nonlinearity observed for the water linkages of Klentaq could be one way to reduce the large error on the $\Delta N_w$ values for Klentaq. Aside from issues concerning differences in hydration changes between the two enzymes, the number of waters released upon DNA binding for both Klentaq and Klenow is very large compared to many DNA binding proteins. For example, the sequence-specific DNA binding of the *lac* repressor, CAP protein, and *Eco*RI endonuclease from *E. coli* only involve the net release of 260 (+/-) 32, 79 (+/-) 11, and 146 (+/-) 4, respectively (18, 19, 30).

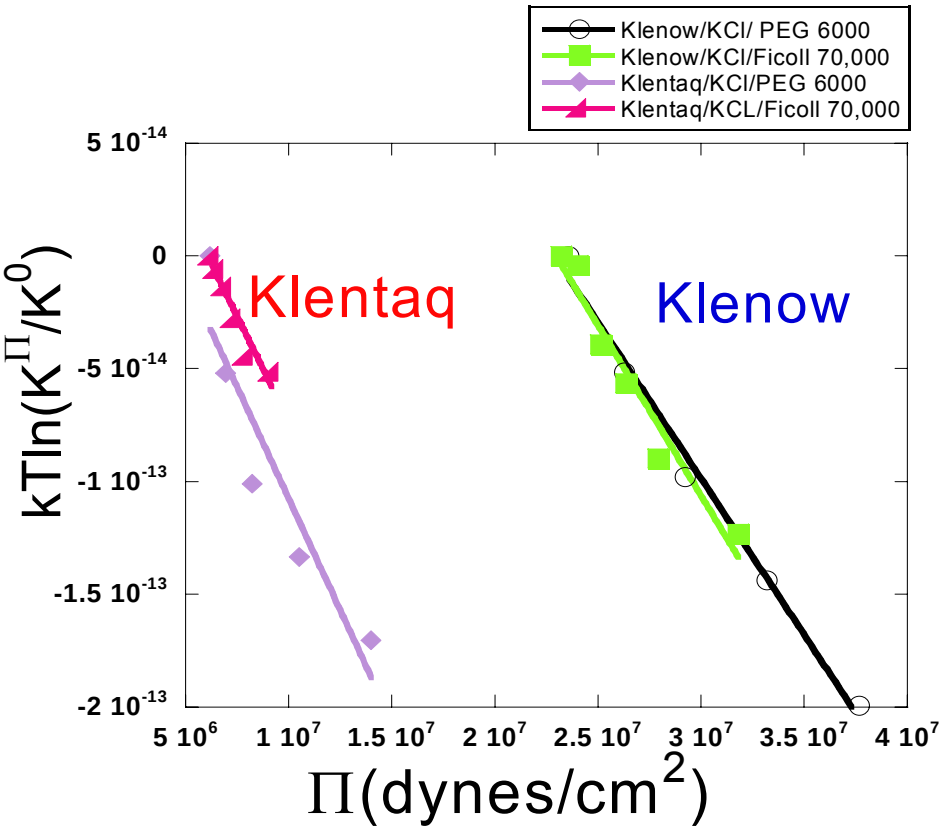


**Figure 10**: Comparison of linkages for Klenow and Klentaq pt-DNA binding under corresponding solution conditions. The slopes appear to be similar. In fact, the linkages done with Ficoll 70,000 translate into $\Delta N_w$ values that are statistically the same and the linkages done in PEG 6000 translate into $\Delta N_w$ values that are close to being statistically the same (Tables 3 & 4). However, the large error in the $\Delta N_w$ values for Klentaq make it difficult to assess any similarity or difference between the hydration changes in Klentaq and Klenow. Also, the non-linearity for linkages done with Klentaq is apparent when compared to the linkages for Klenow.

**Hydration Changes for Klentaq at 65°C**

Osmotic stress was also performed for 63/70 mer DNA binding of Klentaq at 65°C to assess the role of hydration changes in the observed thermodynamic profile for Klentaq (Table 3). Vapor pressure osmometry at 25 º had to be augmented to evaluate the osmotic pressure of high-temperature solutions, because the Wescor VPO only makes measurements at 25º C. Michel and Kaufmann (20, 21) found that the osmotic pressure of PEG 6000 solutions varies quadratically with concentration and linearly with

temperature. For a given concentration of PEG 6000 in pure water, Michel and Kaufmann's measurements on a VPO showed linearity between temperature and ∏ over a temperature range from 25-65 °C. Concentrations ranging from 0.1-0.4 g PEG 6000/g $H_2O$ showed this linear behavior over the temperature range (25-65 °C) (20). Years later, Michel derived an equation that modeled how the ∏ of PEG 8000 solutions varies quadratically with concentration and linearly with temperature. It can written in the form:

$$\prod(\text{dyne/cm}^2) = (-1.31 \text{ X } 10^6 \text{ G}^2 \text{ T}) + (141.8 \text{ X } 10^6 \text{ G}^2) + (4.05 \text{ X } 10^6 \text{ G}) \quad \textbf{Eq. 2}$$

Where ∏ is the osmotic pressure, G = weight percent (g PEG/g $H_2O$), and T is temperature (20, 21, 22). Using a VPO, Michel measured the ∏ of an extensive range of PEG 8000 solutions over a temperature range of 5-40 °C, and he predicted the measurements using the above equation very accurately; the difference between predictions and measurements for almost all concentrations over the temperature range was less than 3 % (21).

For the osmotic stress of Klentaq at 65º, Eq. 2 was used to calculate the ∏ of PEG 6000 solutions in pure water at 65°C for a concentration range of 0.05-0.25 g PEG/g $H_2O$. Eq. 2 should be valid for PEG 6000 solutions. The molecular weight of PEG preparations are only an average of the polymer weights within the sample, and ∏ of equivalent %(w/v) solutions of a PEG 8000 and PEG 6000 did not show significant differences in this study (Table 2). Therefore Eq. 2 should be an accurate predictor of the ∏ for PEG 6000 solutions, especially since the relationship between ∏ and temperature is apparently linear up to 65 °C (20). Since PEG 6000 was added to a base buffer containing 125 mM KCl, 5 mM $MgCl_2$, and 10 mM Tris for equilibrium titrations at 65

ºC, ∏ values were approximated by adding the empirical ∏ of the base buffer at 25 ºC to the calculated ∏ of PEG 6000 in pure water at 65 °C. The dependence of the $K_d$ measured at 65 ºC on these approximated ∏ values was analyzed to provide an estimate of the $\Delta N_w$ for pt-DNA binding of Klentaq at 65 º C. However, the combination of PEG 6000 and base buffer solutes in solution is likely to have significant synergistic effects on the osmotic pressure (21), and thus it was necessary to assess how dramatically the $\Delta N_w$ value would be influenced by neglecting synergistic effects. Synergism means that two agents interact to produce an effect that is larger than the individual effects. The existence of synergism for PEG 6000 and the base buffer solutes in solution would result in the empirical ∏ of PEG 6000 in a base buffer solution being larger than the sum of the individual osmotic pressures of the base buffer and pure aqueous PEG 6000. Since synergism is expected to be greater at lower temperatures (11), the synergism at 25 ºC was determined for PEG 6000 and base buffer solutes to provide a maximum estimate of the synergism at 65 ºC. Table shows 5 shows the synergism for the combination of PEG 6000 and base buffer solutes at 25 ºC, and Figure 11. shows the dependence of synergism on % wt. PEG.

Table 5: Synergism for PEG 6000 solutions at 25 °C

| % wt (g PEG/g $H_2O$) | ∏ of pure aqueous PEG (Calculated) | ∏ of base buffer | Empirical ∏ of PEG in base buffer | Synergism |
|---|---|---|---|---|
| 0 | 0 | 6.54 | 6.54 | 0 |
| 5.2 | 0.39 | 6.54 | 7.22 | +.29 |
| 11 | 1.36 | 6.54 | 8.76 | +.86 |
| 18 | 3.24 | 6.54 | 11.14 | +1.36 |
| 25 | 6.38 | 6.54 | 14.64 | +1.72 |

***All ∏ measurements in units of atmospheres**

**Table 5**: This table shows the approximate synergism for PEG 6000 solutions ranging from 0-0.25 g PEG/g $H_2O$ at 25 °C. All osmotic pressures are in units of atmospheres. The base buffer without PEG has an empirical ∏ of 6.54 atm and contains 125 mM KCl, 5 mM $MgCl_2$, and 10 mM Tris at pH 7.9. The values in the table for the ∏ of pure aqueous PEG were calculated with an equation that is known to accurately predict the ∏ of PEG solutions at 25 °C (13). For PEG 6000, the equation can written in the form: $\mathbf{\prod (dynes/cm^2) = (4.1333 \times 10^4)(\%wt) + (4.96 \times 10^3)(\%wt)^2 + (4.464 \times 10^2)(\%wt)^3}$, where ∏ is given in dynes/$cm^2$ and %wt is the weight percent in (g PEG/g $H_2O$) (13). The synergism is calculated by taking the difference between the empirical ∏ for PEG 6000 in base buffer, and the sum of the calculated ∏ for pure aqueous PEG and the ∏ of the base buffer. Notice the synergism increase as the %wt increases.

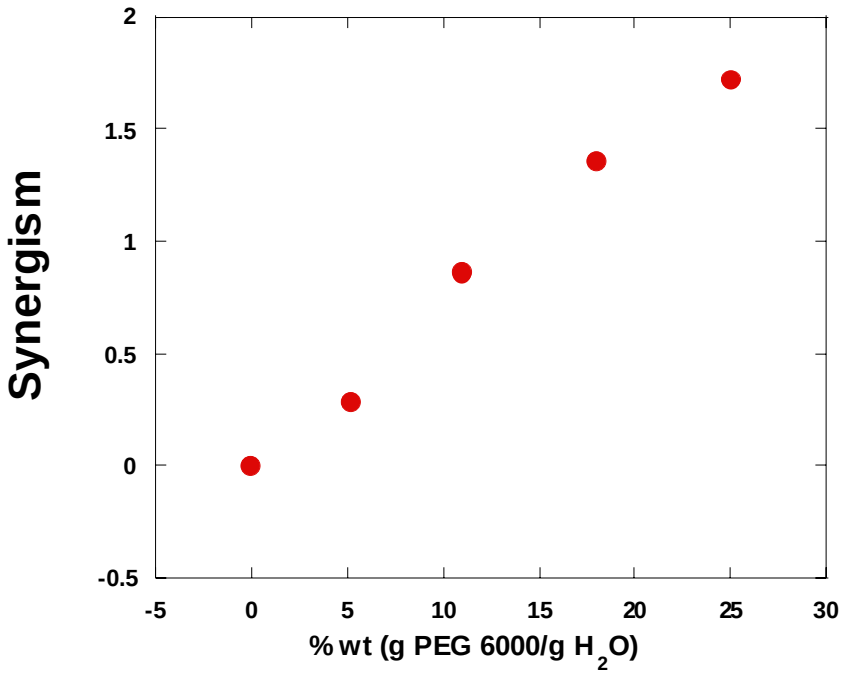


**Figure 11:** Plotted here is the dependence of synergism on the % wt of PEG 6000 solutions. The data for this plot were taken from Table 5. As higher concentrations of PEG 6000 are combined with a buffer containing 125 mM KCl, 5 mM $MgCl_2$, and 10 mM Tris, pH 7.9, the difference between the ∏ of the PEG/buffer combinations, and the sum of the ∏ of pure aqueous PEG and the ∏ of the buffer, increases positively.

A PEG-induced water linkage that doesn't take into account synergism, would use osmotic pressure values on the x axis that would be equal to the sum of the base buffer ∏ and ∏ values of % wt. PEG solutions in pure water. In order to take into account synergism, the synergism for each % wt.PEG/base buffer combination could be added to ∏ values used for the water linkage that disregards synergistic effects. Synergism varies with % wt. PEG and temperature; therefore, the slope of the water linkage is likely to vary with the magnitude of the synergism. Water linkages derived from using estimates of minimum (no synergism) and maximum synergism (synergism at 25 ºC) are in Figure 12, and are labeled as non-synergistic and synergistic.

Figure 12 shows a large water release of 1488 (+/-) 132.8 for the non-synergistic linkage, and 1084 (+/-) 146.5 waters for the synergistic linkage. The uncertainty in determining osmotic pressure, and the large error in the $\Delta N_w$ values introduces significant uncertainties for the hydration changes recorded here at 65 ° C. However, the very large $\Delta N_w$ values likely indicate that the macromolecular hydration change for Klentaq upon binding DNA at 65 ° C is larger than the one at 25 ° C. Although synergism seems to decrease the slope of the water linkages, thus lowering the measured water release, it is doubtful that synergistic effect on the slope would be much greater than shown in Fig 12, because synergism typically decreases with temperature. Also, there would have to be very large errors in the calculations of synergism presented here, for the actual synergism to shift the linkages in Fig. 12 to slopes low enough to translate into a $\Delta N_w$ smaller than ~621 waters.

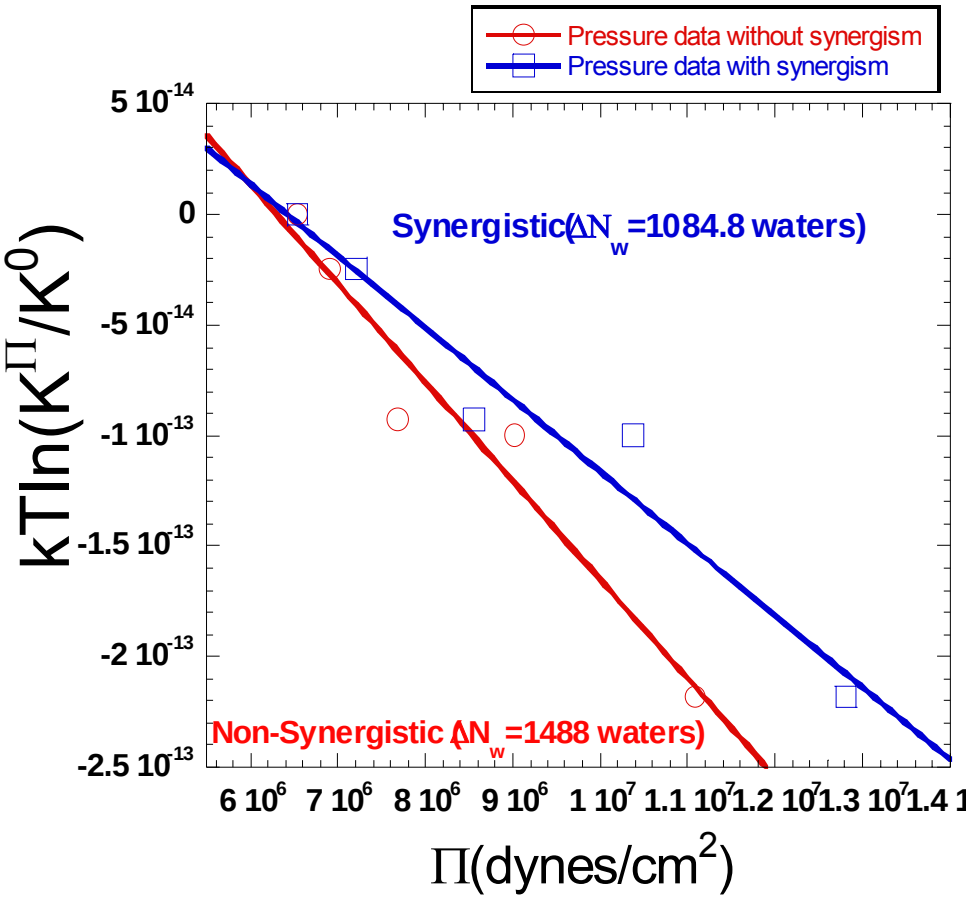


Figure 12: Water linkage plots for Klentaq binding to 63/70 mer DNA at 65 °C. 63/70 mer DNA had to be used because the shorter 13/20 mer DNA would melt under these high-temperature conditions. Klentaq was osmotically stressed with PEG 6000 in a solution of 125 mM KCl, 5 mM $MgCl_2$, pH 7.9. The plots show that Klentaq releases a large amount of water at 65°C. The ∏ values of the red plot (Non-synergistic) are derived from adding the ∏ of the base buffer to the ∏ values of PEG 6000 in pure water calculated by Eq. 2. The empirical ∏ values that would be measured at 65°C might be significantly greater than the ∏ values used for the red plot due to synergism. Therefore, ∏ values that approximate the effect of synergism at 65°C were derived and used for the blue plot (Synergistic). Synergism is discussed in the text above. It is likely that Klentaq releases over a 1000 waters at 65°C.

## Discussion

Klentaq and Klenow are the large fragment domains of the thermophilic/mesophilic pair of Type I DNA polymerases from *Thermus aquaticus* and *Escherichia coli*. Despite their mutual family membership and almost identical three-dimensional structures, Klentaq and Klenow differ significantly in their DNA binding properties (10,11). Differences between the DNA binding properties of Klentaq and Klenow are seen in the salt dependencies, thermodynamics, and structural preferences of their DNA binding (10, 11, Wowor *et. al*., in preparation). In this study, the participation of water in the DNA binding of Klentaq and Klenow was assessed using the osmotic stress technique (13).

**Hydration Changes for the DNA binding of Klentaq and Klenow**

When the osmotic pressure of the bulk solution is increased by adding solutes, processes that involve the release of water from solute inaccessible regions are favored, while those involving the uptake of water are inhibited (13). DNA-binding by both Klentaq and Klenow become more favorable as the $\prod$ of the solution is raised. This means that the binding of DNA by these polymerases involves a net release of water to the bulk solution (13). A net release of water is expected for DNA-protein interactions because a sizable dehydration of both molecules accompanies binding (30). The hydration changes accompanying the formation of the DNA-protein complex for Klentaq of ~621 released waters, and for Klenow of ~489 released waters are large compared to hydration changes accompanying sequence-specific complex formation for many DNA-binding proteins, such as the *lac* repressor, CAP protein, and *Eco*RI from *E. coli* (18,1 9, 30). The binding to non-specific DNA sites by *E. coli lac* repressor, CAP protein, and

*Eco*RI involves the release of less waters compared to sequence-specific DNA binding by these same proteins (18, 19, 30). The crystal structure of *Eco*RI shows that when the enzyme is complexed with its recognition sequence, GAATTC, there are direct protein-DNA contacts with no intervening water (31). From a study on the osmotic dependence of the difference between specific and nonspecific binding of *Eco*RI (25), Rand *et. al* proposed that a full layer of water is retained at the interface between DNA and protein surfaces for the nonspecific complex (28). Although Klentaq and Klenow are primarily non-sequence specific DNA binding proteins, the differences between water participation in sequence-specific and non-sequence specific DNA binding for sequence-specific DNA binding proteins raises interesting questions about Klentaq and Klenow: What mechanisms result in such a large release of water for Klentaq/Klenow? Is any water sequestered at the protein-DNA interfaces? Could the DNA structural preferences and large release of water for Klentaq/Klenow be reflected in a tight fitting of complementary structures (26)?

Changes in macromolecular hydration are often associated with the change in solvent-accessible surface (ΔASA). Although the correlation between macromolecular hydration changes and ΔASA doesn't always hold (13), making this correlation for the DNA binding of Klentaq and Klenow is potentially meaningful because there are already ΔASA values for these proteins calculated from their X-ray crystal structures (PDB 4KTQ and PDB 1KLN), which can be used for comparison. ΔASA can be calculated from osmotic stress data by using an estimate that one water molecule occupies 7-10 $Å^2$ of protein surface, and using the equation:

$$\Delta N_w \text{ X } (7\text{-}10\ Å^2) = \Delta ASA \qquad \textbf{Eq 3}$$

The binding of Klentaq to primed-template DNA involves a release of ~621 waters to the bulk solution. The calculated ΔASA from osmotic stress would be ~5282 $Å^2$ if 8.5 $Å^2$ is used as the area that one water molecule occupies. This value is 2066 $Å^2$ larger than the 3216 $Å^2$ derived from x-ray crystal structures (10). 3216 $Å^2$ takes into account the entire change in surface area for both the protein and DNA; not only the area buried at the protein-DNA interface, but also area buried due to conformational changes in the protein and DNA (10). However, these surface-only calculations from X-ray crystal structures don't take into account some of the possible contributions to water movement that the osmotic stress technique does. Since the structure-based calculations for Klentaq only take into account the release of surface-bound waters, osmotically stressed waters released from regions outside the first hydration layer aren't accounted for, such as those displaced by the entire volume of bound DNA within the binding cleft. For a macromolecule as big as DNA, these waters could lead to an overestimate in ΔASA calculations from osmotic stress. In fact, the X-ray structure of Klentaq bound to primed-template DNA (13, PDB code 4KTQ), reveals a solute-inaccessible DNA volume DNA of ~9738 $Å^3$ (See Methods). If these additional waters are added to the $\Delta N_w$ calculated from the structure-based ΔASA, the result is very close to that of osmotic stress at ~703 waters. Its seems that for the pt-DNA binding of Klentaq, the large volume of non-surface bound waters displaced by the DNA is a major contributor to the discrepancy seen between ΔASA calculations from osmotic stress measurements and X-ray crystal structures.

The large release of ~489 waters to the bulk solution involved with the pt-DNA binding of Klenow would indicate a ΔASA of ~4157 $Å^2$, assuming one water molecule

occupies 8.5 $Å^2$ of macromolecular surface. This change is 1417 $Å^2$ larger than the ΔASA of 2740 $Å^2$ observed by x-ray crystallography for the burial of surface area at the interface of Klenow bound to 10/13 mer DNA (5, PDB code 1KLN,16 ). The approximate solute-inaccessible volume of DNA involved for the pt-DNA binding of Klenow is 9774 $Å^3$ (See DNA volume calculations from x-ray crystal structures). Dividing this volume by 30 $Å^3/H_2O$ indicates a displacement of ~325 waters by the DNA. Using Equation 3 with the same assumptions as above, including ~325 non-surface bound waters for the ΔASA calculations from osmotic stress would lead to an overestimate of 2762 $Å^2$ for the ΔASA calculated by osmotic stress. This overestimate is much larger than the observed discrepancy of 1414 $Å^2$ observed between ΔASA values derived from x-ray crystallography and osmotic stress. Unlike with the pt-DNA binding of Klentaq, it appears that for the pt-DNA binding of Klenow, the observed discrepancy between ΔASA calculations from osmotic stress measurements and x-ray crystals cannot be resolved by taking into account the displacement of non-surface bound waters by the DNA.

For pt-DNA binding, the $\Delta N_w$ values for Klentaq appear to be larger than the $\Delta N_w$ values for Klenow if the statistical error is disregarded. However, the nonlinear dependence of binding affinity on induced $\prod$, observed for water linkages with Klentaq seems to be causing large errors in the $\Delta N_w$ translated from water linkage slopes. The error windows for many of the $\Delta N_w$ values of Klentaq are large enough to overlap with the comparatively smaller error windows for the $\Delta N_w$ values of Klenow. By seeing no statistical difference in the $\Delta N_w$ values for Klentaq and Klenow (Tables 3 & 4), it is difficult to assess any difference in the overall hydration changes between these enzymes.

However, the greater linearity observed for water linkages with Klenow (Fig. 9 and 10) compared to those with Klentaq presents a potential difference in the behavior of these enzymes under induced osmotic pressure. With higher precision data for Klentaq, and possibly fitting Klentaq data non-linearly, a better comprehension of the differences in how water participates in the DNA binding by these enzymes could be gained.

The $\Delta N_w$ for Klentaq binding to 20/20 mer DNA indicates a release of ~167 more waters than the binding to 13/20 mer DNA (Table 3 and Fig. 8). It could be that the larger volume of 20/20 mer DNA and higher number of contacts between the binding site and DNA. However, the large errors in the $\Delta N_w$ values for Klentaq make it difficult to assess this difference in water release with much certainty, but more osmotic stress measurements with 20/20 mer DNA may reveal whether the difference is even significant.

The hydration changes measured for Klentaq pt-DNA binding at 65 ºC indicate a large release of water associated with binding of ~1084-1488 waters. Since the Wescor VPO only measure osmotic pressures at 25 ºC, the osmotic pressures used for the water linkages at 65 ºC had to be calculated. Since synergism is likely to exist between the KCl present in the base buffer and PEG 6000 (21), it was risky to only calculate the osmotic pressure by adding the calculated ∏ of pure aqueous PEG 6000 to the base buffer ∏. The existence of synergism at 65 º C would cause a combination of KCl and PEG 6000 in solution to have a higher empirical ∏ than the result of summing the base buffer ∏ and pure aqueous PEG 6000 ∏. As is seen in Figure 12, the dependence of DNA binding affinity on ∏ would be dependent on whether synergism actually exists between PEG 6000 and ∏ at 65 ºC. The reason for this is that synergism varies with %wt PEG (Fig.

11), and therefore adding values of synergism to the ∏ values calculated for the absence synergism, results in a non-uniform shift in ∏. It is likely that the ∏ values for the synergistic and non-synergistic linkages result from maximum and minimum estimates of the synergism, and therefore it is likely that the actual dependence of binding affinity on ∏ is close to the two dependencies seen for the synergistic and non-synergistic linkages. It then seems that the water linkages at 65 ºC indicate a larger hydration change for Klentaq DNA binding at 65 ºC than 25 ºC.

A larger water release at 65 ºC compared to 25 ºC for Klentaq DNA binding, has interesting implications for the role of water in the thermodynamic driving forces involved in the binding reaction because the release of a large amount of water increases the entropy of a system (16). Datta and LiCata (2003) have performed equilibrium DNA binding experiments with Klentaq using both fluorescence anisotropy and isothermal titration calorimetry and determined, as a function of temperature, the core thermodynamic quantities for this interaction ($\Delta G$, $\Delta H$, $\Delta S$, $\Delta C_p$) (10). The measurement of the temperature dependence of the DNA binding equilibrium, using fluorescence anisotropy, allowed for determination of van't Hoff enthalpies ($\Delta H_{vH}$) at different temperatures, by interpreting a free energy vs. temperature curve ($\Delta G$ vs. T) with Gibbs-Helmholtz analysis. Agreement between van't Hoff enthalpies and enthalpies measured directly on an isothermal titration calorimeter, is important to confirming the thermodynamics for reactions, because differences between van't Hoff and calorimetric enthalpies and heat capacities ($\Delta C_p$) have been observed for a large number of systems. For Klentaq DNA binding, the temperature dependence of the van't Hoff and calorimetric enthalpies and heat capacities agree quite well (10). The thermodynamic

parameters derived from Gibbs-Helmholtz analysis are used here to assess the contribution of hydration changes to characteristics of the observed thermodynamic profile for Klentaq DNA binding. The temperature dependence of the thermodynamic parameters ΔH, ΔG, and TΔS of Klentaq are graphed in Figure 13. The more negative the change in free energy (ΔG) is for a reaction, the more favorable the reaction is, and the ΔG is related to the entropy (ΔS) and enthalpy (ΔH) change of a reaction by ΔG = ΔH- TΔS. Figure 13 shows that for Klentaq DNA binding, the temperature-dependent enthalpy and entropy deviations are far larger than the temperature-dependent deviations in the ΔG. Klentaq DNA binding is enthalpy-driven at high temperatures and entropy-driven at low temperatures. The more positive entropy change at lower temperatures shows that the system is becoming more disordered with the DNA binding of Klentaq, while at the negative entropy change at higher temperatures shows that the system is becoming more ordered. In fact, TΔS at 65 ºC is 32 kcal/mol more negative than TΔS at 25 ºC (10). This raises the question of what molecular processes associated with the DNA binding of Klentaq contribute to the difference in entropy changes at higher and lower temperatures? The release of a large amount of water with a macromolecular process increases the entropy of a system (16). If differences in the amount of water released were responsible for the temperature-dependent entropy changes observed for Klentaq DNA binding, than it would be expected that Klentaq DNA binding would release less waters at 65 ºC than at 25 ºC. However, Klentaq DNA binding appears to release more waters at 65 ºC than at 25 ºC. Therefore, differences in hydration changes between binding at lower and higher temperatures is not likely to be a major contributor to the strong temperature-dependence of the entropy change for Klentaq DNA binding.

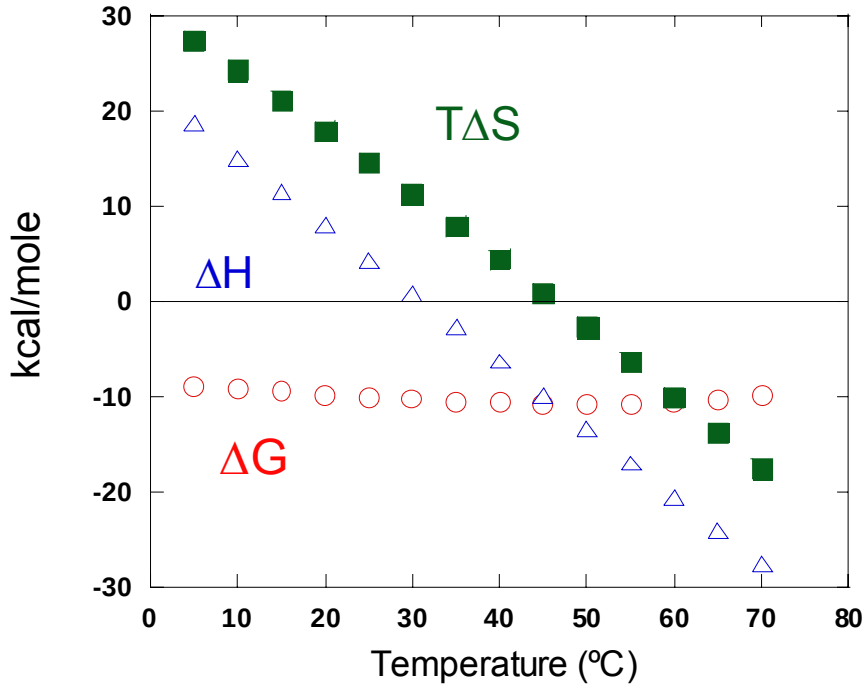


**Figure 13:** Temperature dependence of the thermodynamic parameters ΔH, ΔG, and TΔS of DNA binding by Klentaq. DNA binding by Klentaq is entropy-driven at lower temperatures and enthalpy-driven at higher temperatures. The TΔS at 65 º C is 32.16 kcal/more negative than the TΔS at 25 ºC. Data from reference 10.

The osmotic stress performed for this study shows that water plays a significant role in Klentaq and Klenow DNA binding. Raising the osmotic pressure of the solution by adding non-interacting solutes (osmolytes) increases the binding affinity of Klentaq and Klenow for DNA. The solutes of the bulk solution are excluded from many hydration spaces on the proteins, and therefore osmotically stress the water in these spaces. The movement of stressed waters to the bulk solution is favored, and since Klentaq DNA binding involves the release of water, this process is thermodynamically favored along with the release of water. The large $\Delta N_w$ values for Klentaq and Klenow DNA binding compared to the $\Delta N_w$ values for many other DNA binding proteins suggests that the

hydration changes may be especially important to DNA binding by Klentaq and Klenow in the cell, where the osmotic pressure is very high (16).

## References


1. Chien, A., Edgar, D. B., and Trela, J. M. (1976) *J. Bacteriol.* **127**, 1550-1557
2. Kaledin, A. S., Sliusarenko, A. G., and Gorodetskii, S. I. (1980) *Biokhimiya* **45**, 644-651
3. Lawyer, F. C., Stoffel, S., Saiki, R. K., Myambo, K., Drummond, R., and Gelfand, D. H. (1989) *J. Biol. Chem.* **264**, 6427-6437
4. Lawyer, F. C., Stoffel, S., Saiki, R. K., Chang, S. Y., Landre, P. A., Abramson, R. D., and Gelfand, D. H. (1993) *PCR Methods Applications* **2**, 275-287
5. Perler, F. B., Kumar, S., and Kong, H. (1996) *Adv. Protein Chem.* **48**, 377-435
6. Perler, F. B., Kumar, S., and Kong, H. (1996) *Adv. Protein Chem.* **48**, 377-435
7. Barnes, W. M. (1992) *Gene* (*Amst.*) **112**, 29-35
8. Korolev, S. Nayal, M., Barnes, W.M., DiCera, E. and Waksman, G. (1995) *Proc. Natl Acad. Sci. USA.* **92**, 9264-9268.
9. Brock,T.D. (1974) In Buchanan and Gibbons (eds), *Bergey's Manual of Determinative Bacteriology*, 8th Edn. Williams and Wilkins, Baltimore, MD, p. 285.
10. Datta, K. and LiCata, V.J. (2003) *Nucleic Acids Research.* **31(19)**, 5590-5597.
11. Katta, K. and Vince J. LiCata. (2003). *Journal of Biological Chemistry.* **278 (8)**, 5694-5701

12. Datta, K., Wowor, A.J., Richards, A.J., and LiCata, V.J. (2006) *Biophysical Journal*. **90,** 1739-1751.

13. LiCata, V.J., and Allewell, N.A. (1997) *Biochemistry.* **36,** 10161-10167

14. *Joe Dundas, Zheng Ouyang, Jeffery Tseng, Andrew Binkowski, Yaron Turpaz, and Jie Liang. 2006. CASTp: computed atas of surface topography of proteins with structural and topographical mapping of functionally annotated residues. Nucl. Acids Res., 34:W116-W118.*

15. Bhat, R, and Timasheff, S.N. (1992) *Protein Science.* **1,** 1133-1143.

16. Parsegian, VA, Rand, RP, and Rau, DC. (1995) *Methods Enzymol*. **259**, 43-94.

17. Bloomfield, V.A. and Wenner, J.R. (1999) *Biophys J.* ***77,*** 3234-3241.

18. Fried, M.G., Stickle, D.F., Smirnakis, K.V., Adams, C., MacDonald, D., and Ponzy, L. (2002) *J. Biol. Chem.* **277**, 50676-50682.

19. Vossen KM, Wolz R, Daugherty MA, and Fried MG. (1997) *Biochemistry.* **36,** 11640-7.

20. Michel, B.E. (1983) *Plant Physiol.* **72**, 66-70. Michel, B.E., and Kaufmann, M.R. (1973) *Plant Physiol*. **51**, 914-916.

21. Michel, B.E. (1983) *Plant Physiol.* **72**, 66-70.

22. Parsegian, V.A., Rand, R.P Fuller, N.L., and Rau D.C. (1986) *Methods Enzymol*. **127,** 400-416.

23. Cohen, J.A, and Highsmith, S. (1997) *Biophysical Journal*. **73**, 1689-1694.

24. Fried, M.G., Stickle, D.F., Smirnakis, K.V., Adams, C., MacDonald, D., and Ponzy, L. (2002) *J. Biol. Chem.* **277**, 50676-50682.

25. Sidorova, N.Y., and Rau, D.C. (2004) *Biophysical Journal.* **87,** 2564-2576.

26. Datta, K., Wowor, A.J., Richards, A.J., and LiCata, V.J. (2006) *Biophysical Journal*. **90,** 1739-1751.

27. Colombo, M.F., Rau, D.C., and Parsegian, V.A. (1992) *Science* **256,** 655-659.

28. Rand, R.P., Parsegian, V.A., and Rau, D.C. (2000) *Cellular and Molecular Life Sciences.* **57**, 1018-1032.

29. Korolev, S. Nayal, M., Barnes, W.M., DiCera, E. and Waksman, G. (1995) *Proc. Natl Acad. Sci. USA.* **92**, 9264-9268.

30. Robison, C., and Sligar, S. (1998) *Proc. Natl. Acad.Sci.* USA, **95**, 2186-2191.

31. McClarin, J.C., Frederick, C.A., Wang, B.C., Greene, P., Boyer, H.W., and Rosenberg, J.M. (1986) *Science*. **234:** 1526-1541.

32. Heyduk, T., and Lee, J.C. (1990) *Proc. Natl. Acad. Sci. U.S.A.* **87,** 1744-1748

33. Heyduk, T., Ma, Y., Tang, H., and Ebright, R.H. (1996) *Methods Enzymol.* **274.** 492-503